analytical chemistry

Technical Note

pubs.acs.org/ac

Quantitative Study of the Dynamic Tumor–Endothelial Cell Interactions through an Integrated Microfluidic Coculture System

Chunhong Zheng, Liang Zhao, Gui'e Chen, Ying Zhou, Yuhong Pang, and Yanyi Huang*

College of Engineering and Biodynamic Optical Imaging Center (BIOPIC), Peking University, Beijing 100871, China

ABSTRACT: The interaction between tumor and endothelial cells is crucial to cancer metastasis and angiogenesis. We developed a novel microfluidic device to assess the cell–cell interaction quantitatively at the single cell resolution. This integrated chip offers 16 coculture experiments in parallel with controllable microenvironments to study interactions between cells dynamically. We applied this approach to model the tumor invasion using Hela cells and human umbilical vein endothelial cells (HUVECs) and monitored the migration of both. We observed the retreatment of HUVECs upon the approach of Hela cells during coculture, indicating that the interaction between two cells was mediated by soluble factors. This interaction was further analyzed through quantitatively processing the phase-contrast microscopic time-lapse images of each individual coculture chamber. We also confirmed this paracrine effect by varying the frequency of medium change. This microfluidic technique is highly controllable, contamination free, fully automatic, and inexpensive. This approach not only offers a unique way to quantitatively study the interaction between cells but also provides accurate spatial-temporal tunability of microenvironments for cell coculture. We believe this method, intrinsically high-throughput and quantitative, will greatly facilitate the study of cell–cell interactions and communications.

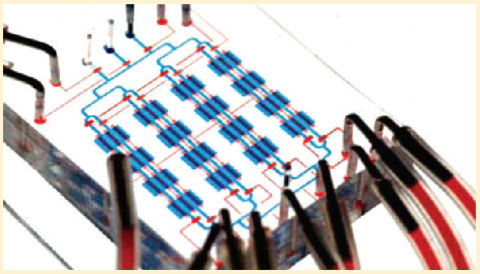

Tumor metastasis causes the death of most cancer patients. Several critical steps are involved in the process. Metastasis starts when the tumor cells trespass the normal tissue surrounding the primary tumor. Then, they enter and migrate along the stream of lymphatic or blood circuit and colonize and grow at a new site.[1] During this process, the first and foremost event is the tumor cell invasion governed by cell–cell interaction. Quantitative studying of the interaction between tumor and tissue cells is highly desirable because this interaction plays a critical role in many processes related to cancer growth and progression,[2] including angiogenesis and metastasis. To investigate such interactions in vitro, it is necessary to create a coculture system, in which two types of cells can grow together and interplay between them can be observed and further analyzed. The goal of a coculture system is to mimic the in vivo microenvironment of real organisms. Simply mixing different types of cells can create a simple coculture system, and seeding density can modulate the degree of cell interaction. However, under the real physiological conditions, cells usually form colonies and the long-range interaction often started first through many soluble factors such as cytokines. Hence, a practical coculture system requires the capability to reconfigure the format of the culture chamber: it can culture and treat different types of cells individually to form the colonies and can also bring these cells together to perform the coculture. A common practice is to separate different cells using a porous membrane during coculture.[3−5] However, such approaches typically lack accurate control of spatial and temporal parameters, which are of pivotal importance in biological systems.

Recent advances in surface chemistry and micropatterned cell culture have greatly improved the controllability and precision of heterotypic cell coculture.[6−12] These techniques focus on modifying the substrate, and thus, the localized cell attachment can be controlled precisely and dynamically. Nevertheless, surface functionalization requires extra effort and time. In addition, most investigation of cell communication has been done under static conditions, lacking dynamic information of the process. Recent developments in microfabrication and microfluidic technologies have shown great potential to overcome these limitations, allowing precise spatial-temporal control and mimicking an in vivo microenvironment.[13−17] Selective patterning has been realized using microfluidic channels combined with electrochemical desorption of self-assembled monolayers,[18] creating a controllable device for cell coculture.[19] Cocultures can also be performed using micro-stencil[20] and extracellular matrix patterning,[21] as well as microwells.[22] With the help of microfluidic devices, precisely controlled coculture could also be created by laminar flow[23,24] or by passive surface tension driven pumping.[25] Recently, interactions between cocultured Hela cells and human umbilical vein endothelial cells (HUVECs) have been studied in miniature devices.[26] Soluble factor effects have also been investigated using a microfluidic chip.[27] However, this technique requires two complementary substrates with precultured cells. Besides, the mechanical assembling process is also harmful to cells at the edge of the substrates.

Received: December 2, 2011
Accepted: January 21, 2012
Published: January 21, 2012

dx.doi.org/10.1021/ac2032029 | *Anal. Chem.* 2012, 84, 2088–2093

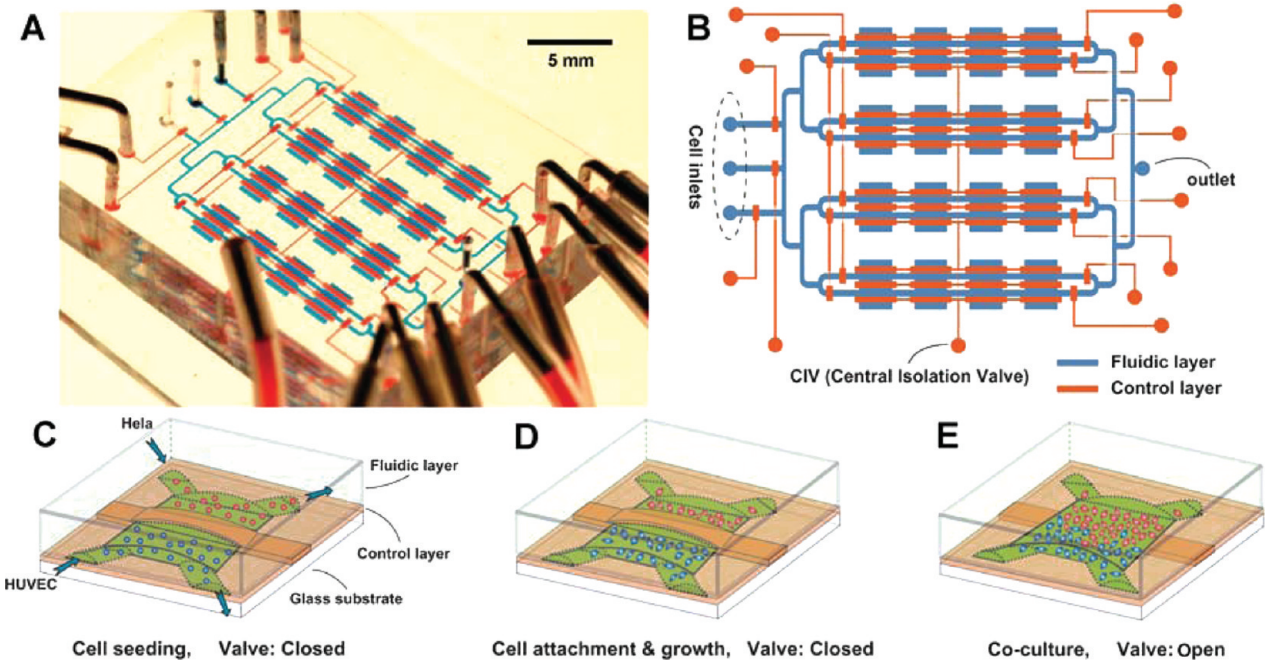

Figure 1. The design of the microfluidic coculture device. (A) The macro image of a coculture chip. The control valve and fluidic channels were introduced with red and blue dyes, respectively. (B) Schematic diagram of the chip design. (C) Hela and HUVEC cells were introduced from different inlets to culture chambers in the fluidic layer. Each culture chamber can be physically separated as two compartments by a pneumatic central isolation (CI) valve. (D) Cells attached and grew in the chamber, and the CI valve was kept closed to ensure the separated culture. (E) To form coculture, the CI valve was open to make the central area of chamber available for cells to migrate and to interact with each other.

In this paper, we present an integrated microfluidic device to quantitatively study the tumor−endothelium interaction. This chip-based device allows fully automatic coculture of two different types of cells. We observe the interaction between them through real-time monitoring and analyzing the migration of cells. We also performed both monoculture and coculture by adjusting the valve configurations of the device. Each device has 16 (4 × 4) coculture assaying chambers, through which the control experiments can be conducted simultaneously under the same conditions. We also test the soluble factor effect during coculture by controlling the frequency of media change. To ensure the reproducibility and robustness of the experiments, we carry out all operations on-chip, including cell seeding, coculturing, migration monitoring, medium changing, and multiplexed migration analysis.

EXPERIMENTAL SECTION

Fabrication of Microfluidic Devices. The microfluidic devices were fabricated using multilayer soft lithography technology.[28,29] Briefly, control-line mold was made from a 20 μm negative photoresist (SU8-2010, MicroChem, Newton, MA, USA) patterned on a silicon wafer using photolithography. The master mold of fluidic channels was made from positive photoresist (P4620, AZ Electronic Materials, Branchburg, NJ, USA). This mold was rounded after reflow (from 40 to 220 °C, 20 °C/h on the hot plate), and its height was about 20 μm. Then, PDMS (Sylgard 184, Dow Corning, Michigan, USA) was cast on the master to make chips after all molds were exposed to chlorotrimethylsilane (TMCS) vapor for 10 min. PDMS mixture with a ratio of 23:1 was spin-coated onto the control channel mold at 1300 rpm for 60 s, whereas PDMS with a ratio of 5:1 was used to make the fluidic layer of the device. After both of these two layers were cured in an oven at 80 °C for 30 min, PDMS slab on the fluidic layer mold was peeled off and holes were punched. The fluidic slab and control layer were then aligned together and baked at 80 °C for 60 min. The two assembled layers were peeled off from the control channel mold, and then, holes for control lines were punched. Finally, the assembled chip was placed on a glass slide, which was spin-coated with PDMS (ratio 20:1, 1300 rpm for 60 s, and cured at 80 °C for 30 min). The whole device was put in an oven overnight.

Cell Culture. The primary human umbilical vein endothelial cells (HUVECs) were isolated from umbilical cord. HUVECs were typically cultured with Medium 199 (M199, Invitrogen) supplemented with 5% fetal bovine serum (FBS, ScienCell), 1% penicillin−streptomycin (PS, Invitrogen), and 1% endothelial cell growth supplement (ECGS, ScienCell). Hela cells were cultured with Medium RPMI 1640 (RPMI 1640, Invitrogen), supplemented with 10% FBS and 1% PS. All cells were cultured at 37 °C in a humidified incubator containing 5% CO_2. When cells became confluent, they were detached with 0.25% trypsin with 0.1% EDTA (Invitrogen) and centrifuged at 1200 rpm for 3 min. Then, the supernatant was discarded, and cells were resuspended at a density of 2 × 10^7/mL for passaging.

Microscopy Imaging and Cell Culture on Chip. Before loading the cells on-chip, we coated the entire fluidic channels with fibronectin (300 μg/mL, Invitrogen) for 2 h. Then, the cells were loaded through the inlets on chip with tygon tubing. When cells became confluent, the central isolation valves were released and phase-contrast images of cells' migration in each chamber were recorded by an automated microscope (TE2000-E, Nikon) with a monochrome CCD camera (2000R, Qimaging, Canada). The chip was incubated in a homemade miniaturized live-cell culture incubator which was made from plexiglass and fixed on a motorized translational stage (BioPrecision, Ludl Electronic Products Ltd., Hawthorne, NY, USA). This device contained two indium−tin-oxide (ITO)

dx.doi.org/10.1021/ac2032029 | Anal. Chem. 2012, 84, 2088−2093

glass plates on both bottom and top sides of the chip, and the temperature of the two plates were controlled by two PID controllers. This design maintained the temperature inside the chip and avoided water condensation on the top of the device. Water and 5% CO_2 were introduced into the incubator to prevent medium evaporation from the inside of the chip and to ensure that the cells were healthy during the entire experiment. All instruments were controlled by our own program script written in MATLAB (Mathworks, Natick, MA, USA). The cell culture medium in the chip was replaced with preset frequency through pneumatic control.

RESULTS AND DISCUSSION

To study cell−cell interactions quantitatively, a key requirement is to pattern different cells with great spatial and temporal precision. Traditional methods are usually difficult to achieve physical or biochemical control of different types of cells precisely. It is also difficult for them to monitor cell migration behaviors automatically or to mimic the in vivo microenvironment of organisms where tumors inhabit. We designed a microfluidic device (Figure 1A) to achieve compartmentalized cell loading. Figure 1B shows an individual coculture chamber, with two cell-loading compartments and a central isolation (CI) valve in between. While the CI valve was closed, Hela and HUVEC cells were introduced into two compartments, respectively. This loading process for multiple compartments inside a single chip was performed in a single run since the chambers were connected by microchannels in series. After cell loading, the device was mounted on a homemade cell incubator (37 °C, with 5% CO_2) for 2 h to facilitate cell attachment without medium change.

We kept the CI valve closed for another 2 h after the loading step to allow cells to fully attach onto the bottom surface of the culture chambers and to grow to confluence. We then opened the CI valve and created a blank region between the two cell islands. Both HUVEC and Hela cells could migrate out of their originally confined compartment and move into this blank region (Figure 1C−E). Besides the CI valve, the other two valves located on each side were also opened and cells might also move into these new territories (Figure 1B). In each chip, we conducted 16 (a 4 × 4 matrix, Figure 1A,B) pairs of coculture experiments in parallel. By placing different types of cells into these compartments, control experiments could also be done within the same chip under the same conditions simultaneously.

The controllable CI valve provides precise control of the time zero (t = 0) for a coculture system, allowing the accurate investigation of the interaction dynamics between two groups of cells. We captured a series of time-lapse microscopic phase-contrast images of each coculture chamber, after we opened the CI valves and the side valves. Through these images, we monitored the cells' migration process at the single cell resolution. Both collective migration of cells and the trajectories of each cell could be analyzed to unveil the details of interaction between the cells. Figure 2A−D shows the images we took from a single chamber at the time 0 h, 12 h, 24 h, and 36 h, respectively. The leading edges of both cell islands are also shown in the images. At the beginning, a few cells occupied both sides of the marginal area of CI valve, as shown in Figure 2A. This phenomenon was caused by the valve actuation in the chip with multilayer structures. When pressure was applied to the control layer, the elastic PDMS membranes expanded and deflected toward the fluidic channels to block a certain area. At

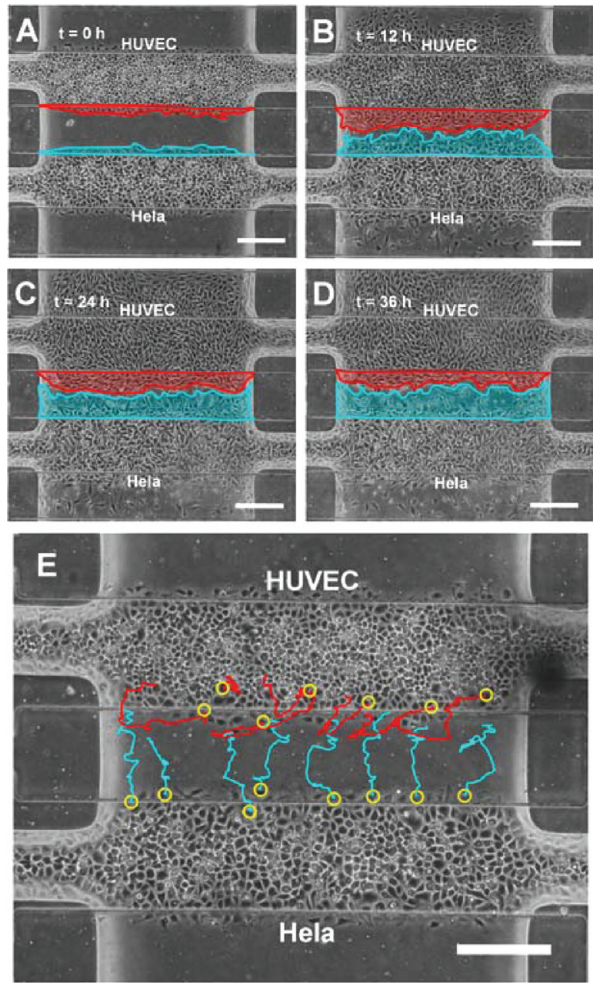

Figure 2. The migration of HUVEC and Hela cells during coculture on-chip. (A−D) Phase-contrast images of the coculture at different times after opening the CI valve. The cells' migration areas from the datum line to the frontiers are depicted by red (HUVECs) and cyan (Hela) lines, respectively. (E) The trajectories of some pioneer cells during the 36 h coculture. The yellow circles indicate the original locations of the single HUVEC and Hela cells. Scale bars: 300 μm.

the edge of the valves, a small portion of space was not covered by the membrane due to the limit of the PDMS membrane deformability, and cells would grow inside this area while the valves were closed.

Our device provided an automatic approach to coculture cells with accurate measurement of cell interactions. To assess the migration of cells, we used the edge of the CI valve as a datum line of cells' movement or coverage. The area between the leading frontier facing the blank region and the datum line has been used as the parameter to measure the collective migration of the cells. Soon after we released the CI valve, cells on both sides started migrating into the blank region, as shown in Figure 2B. The areas covered by different cells were not identical, indicating the difference of their migration speeds. In our case, Hela and HUVECs showed different behaviors of migration. Collectively, HUVECs had higher motility than Hela. In the later stage of the experiment, Hela cells continuously moved forward but HUVECs retreated, as shown in Figure 2C,D. Besides the observation of collective migration, we also tracked the moving trajectories of a few cells at the frontiers, plotted in Figure 2E. These trajectories clearly

dx.doi.org/10.1021/ac2032029 | Anal. Chem. 2012, 84, 2088−2093

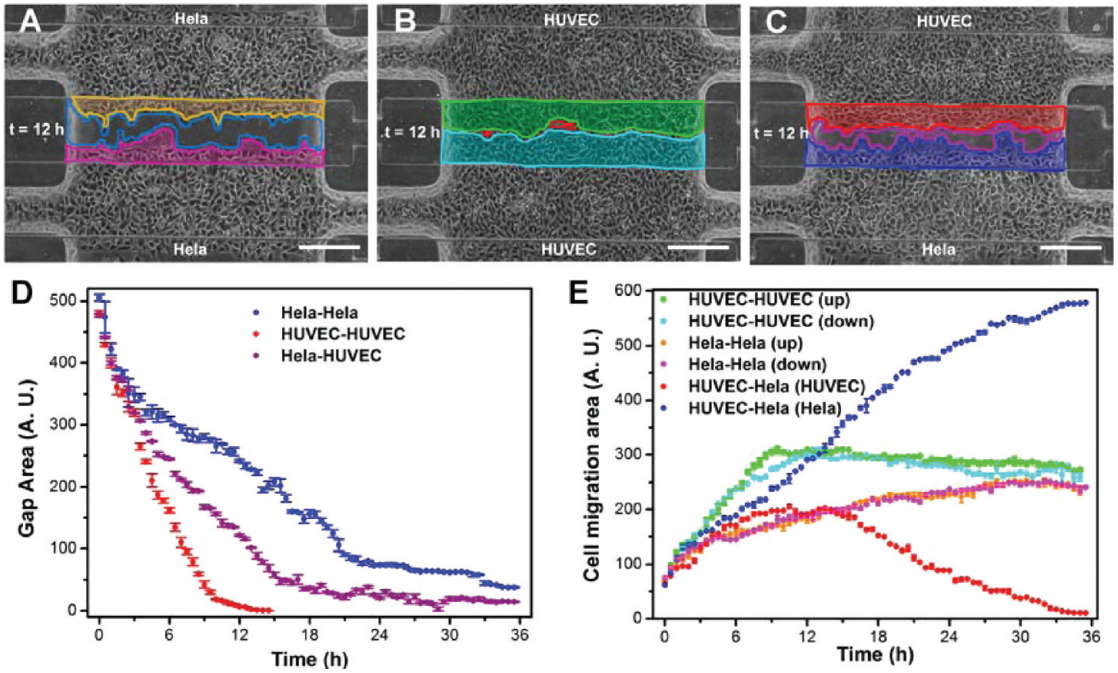

Figure 3. Dynamical analysis of the cell migration during coculture. (A–C) The images of single coculture chambers with Hela–Hela, HUVEC–HUVEC, and Hela–HUVEC coculture, respectively. All images are taken after the 12 h of coculture. For these three cases, the gaps between the two cell islands are depicted as blue, red, and purple lines, respectively. The migrated areas of Hela cells are indicated as orange and magenta lines in (A). The migrated areas of HUVEC cells are indicated as green and cyan lines in (B). The migrated areas of HUVEC and Hela cells are marked as red and blue lines, respectively, in (C). (D) The dynamics of gap closure during the coculture process. Error bars come from the four individual measurements of the gap area in each image. (E) The collective cell migration areas have been plotted as function of time during coculture. The curve colors are the same as marked in (A–C). Scale bar: 300 μm.

showed the retreat of HUVECs and the progressive motion of Hela cells. Some Hela cells would migrate extensively faster than the majority and aggressively penetrate into the HUVEC colony. On the contrary, the migration of HUVECs was uniform and ordered. These observations agreed with previous reports,[26,27] indicating that our device was suitable for cocultivation of different types of cells. Furthermore, culturing cells on-chip also brought many other advantages over conventional approaches. The cells were kept in a closed environment, which allowed the experiment to be conducted in a nonsterilized condition without risk of contamination. The automatic control of the valves inside the chip further eliminated the human interferece of the culture system and required much less reagent consumption.

One of the most important applications of this coculture device is that the dynamical cell–cell interaction can be analyzed and then quantitatively described through time-lapse images taken in situ. The microfluidic chip provided identical replications for each condition, greatly improving the repeatability of the experiments. We measured the migration areas of each side of the cells along the coculture process, as well as the gap in between. The monoculture experiment, which loaded the same cells in both sides of the coculture chamber, was performed for comparison. Figure 3A–C is images taken from three individual coculture chambers at t = 12 h, and the cells loaded in the chambers were Hela–Hela, HUVEC–HUVEC, and HUVEC–Hela, respectively. Figure 3D shows the process of gap closure between the two cell islands. The reduction rate of the gap area in Hela–Hela monoculture is much slower than that of HUVEC–HUVEC, which confirms that the HUVECs can migrate faster than Hela cells. As a compromised consequence, the decreasing rate of the gap area in HUVEC–Hela coculture is between those of the two monoculture controls. In addition, to present the dynamic cell migration, we measured the cell motile area of both cell islands, as shown in figure 3E. In both the coculture and monoculture cases, for every 30 min, the areas from the frontier cells to the datum line were measured four times to quantitatively evaluate the cell migration. In the first 8 h of coculture, both Hela and HUVEC cells migrated from their original place to the blank area at the center. Thereafter, from t = 8 h to t = 15 h, the HUVECs stopped moving forward, shown as a plateau on the corresponding curve, whereas the Hela cells continued to move forward to the HUVECs at a relatively stable speed (Figure 3E). Subsequently, the slope of the HUVEC migration curve became negative while the Hela curve is positive.

From t = 15 h to t = 36 h, HUVECs retreated at a roughly constant speed. It has been reported that the drawing back of endothelial cells would attribute to the injury of endothelial cells caused by some soluble factors produced by tumor cells such as reactive oxygen species.[30] Some researchers also found that contact between tumor cells and endothelial cells could induce overexpression of the endothelial adhesion molecule and then facilitated the tumor cells to stick on the endothelial cells in cancer progression.[5] Interestingly, the migration speed of Hela cells in the Hela–HUVEC coculture was faster than that in the Hela–Hela monoculture. This phenomenon may be attributed to the homotypic contact inhibition of locomotion between the tumor cells themselves. We observed that in Hela–Hela monoculture system, some of the fast migrated Hela cells might contact other Hela cells from opposite sides around t = 4 h. Thus, the Hela cells would redirect their migration routes due to the protrusion inhibition, as reflected as

dx.doi.org/10.1021/ac2032029 | *Anal. Chem.* 2012, 84, 2088–2093

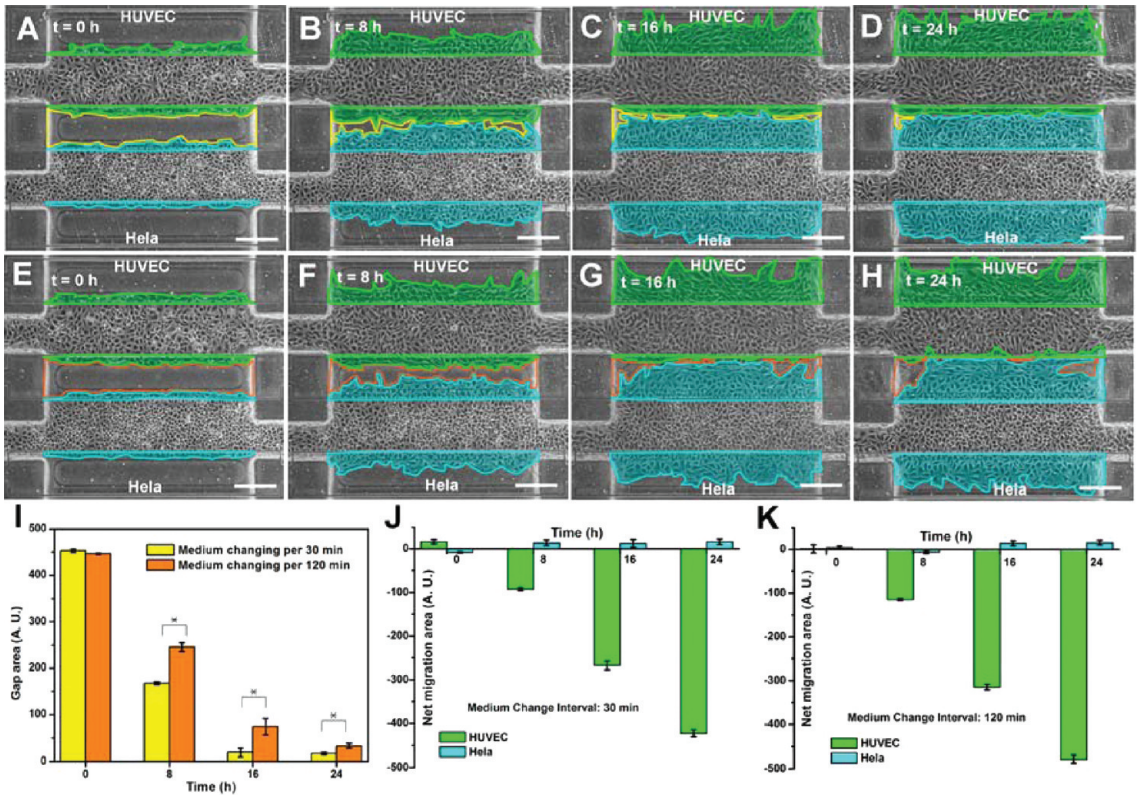

Figure 4. Cell migration with different frequency of medium change. (A–H) Phase-contrast images of cell coculture chamber at the time points of t = 0 h, 8 h, 16 h, and 24 h, respectively. The culture medium was changed every 30 min in (A–D) and every 2 h in (E–H). Yellow and orange lines define the gap boundary between the two cell islands. Green and cyan lines indicate the areas that HUVECs and Hela cells migrated to both sides of the cell islands. Scale bars: 300 μm. (I) The area of the gap between Hela and HUVEC cell islands at different time points. The error bars come from four independent coculture chambers on a single chip. *$p < 0.05$. (J–K) The "net migration" (NM) area at different time points. NM areas indicate the difference between the cell migration area toward the central blank region and that toward the cell-free blank region.

the slope of Hela cell migration decreases in Hela–Hela group compared with the Hela's slope in Hela–HUVEC group shown in Figure 3E. In the coculture case, this inhibition was reduced when confronted with normal cells.[31,32] The ability of monitoring the dynamical migration at the single cell resolution would help us to capture the details of cell–cell interaction with highly quantitative analysis.

To further substantiate the paracrine signal effect in tumor–endothelial cell interaction, we studied cell migration in both coculture and monoculture systems with different frequencies of medium change. Recurrent medium change would eliminate a sort of effects of soluble factors, especially slowly diffusing ones before they reached target cells and triggered the downstream response. Two periodicities of medium change, refreshed every 30 min or 2 h, was tested. More frequent medium change led to less retreatment of HUVECs during coculture (Figure 4A–D), while less frequent medium change facilitated the retreatment (Figure 4E–H). This phenomenon indicates that the HUVECs tend to avoid Hela cells before the physical contact; hence, there are indeed soluble factors secreted by Hela, and the gradient of these factors mediated HUVECs' migration. These cytokine molecules would accumulate in the medium during the coculture process. When we refreshed the chamber with new medium solution, these cytokines were washed away and the HUVECs did not retreat until they confronted Hela cells. We quantitatively measured the gap area between cell islands during the coculture process. Notably, with frequent medium change, the gap area was significantly smaller than that with infrequent refreshment (Figure 4I). In fact, the gap was fully closed after 24 h of coculture with frequent medium change.

In a coculture chamber, each cell island had two frontiers, one facing another cell island and the other facing a cell-free region. Both frontiers moved outward because cells in the island tended to move to any vacant area. We calculated the vector sums of the cell migration area from both frontiers of each island, as shown in Figure 4J,K. We found that the "net migration" (NM) of HUVECs showed an unbalanced migration pattern that the territory covered by cells that migrated toward Hela is much smaller than the area covered by migratory cells toward cell-free region. However, the NM of Hela cells was around zero, indicating that Hela cells moved symmetrically to both sides. This difference between two cells reflected that, compared with HUVECs, Hela cells were less sensitive to the heterotypic contact inhibition of locomotion. With low frequency of medium refreshment, HUVECs has larger NM area due to greater retreatment of HUVEC cells. This quantitative analysis of retreatment also confirms that the soluble factors secreted from Hela cells play a critical role in repelling the endothelial cells in this coculture system.

■ CONCLUSIONS

We have presented a novel method to quantitatively study the cell–cell interactions with a microfluidic coculture system. The interaction between cells can be controlled by monolithically integrated microvalves and the frequency of medium change. With this fully automatic method, a single chip can carry out

dx.doi.org/10.1021/ac2032029 | Anal. Chem. 2012, 84, 2088–2093

multiple experiments in parallel, including control experiments. The interactions between cells can be analyzed by observing the migration at the single cell level in situ. In this study, we demonstrated the coculture of Hela and HUVEC cells, as a model of cell−cell interactions in tumor metastasis. The results show the retreatment of HUVECs when Hela cells approach during the coculture, suggesting significant interactions between these two cells through soluble factors. Moreover, the paracrine effect had been simply substantiated by varying the frequency of medium change on chip. We envision this approach may open a way for investigating cell−cell interactions involved in cancer progression or other biologic systems with advantages of low cost, high integration, dynamic analysis, and full automation.

AUTHOR INFORMATION

Corresponding Author

*E-mail: yanyi@pku.edu.cn.

Notes

The authors declare no competing financial interest.

ACKNOWLEDGMENTS

C.Z. and L.Z. contributed equally to this work. This work is supported by the National Natural Science Foundation of China (20890020, 90913011, 20905004), the Ministry of Science and Technology of China (2011CB809106), and the Fok Ying Tong Education Foundation. We also appreciate Haidian Maternal and Children's Health Hospital for providing HUVECs.

REFERENCES

(1) Steeg, P. S. *Nat. Med.* **2006**, *12*, 895−904.
(2) Wiseman, B. S.; Werb, Z. *Science* **2002**, *296*, 1046−1049.
(3) Rose, S. L.; Babensee, J. E. *Ann. Biomed. Eng.* **2007**, *35*, 1382−1390.
(4) Zengel, P.; Ramp, D.; Mack, B.; Zahler, S.; Berghaus, A.; Muehlenweg, B.; Gires, O.; Schmitz, S. *BMC Cancer* **2010**, 10.
(5) Haddad, O.; Chotard-Ghodsnia, R.; Verdier, C.; Duperray, A. *Exp. Cell Res.* **2010**, *316*, 615−626.
(6) Tourovskaia, A.; Barber, T.; Wickes, B. T.; Hirdes, D.; Grin, B.; Castner, D. G.; Healy, K. E.; Folch, A. *Langmuir* **2003**, *19*, 4754−4764.
(7) Khademhosseini, A.; Suh, K. Y.; Yang, J. M.; Eng, G.; Yeh, J.; Levenberg, S.; Langer, R. *Biomaterials* **2004**, *25*, 3583−3592.
(8) Bhatia, S. N.; Yarmush, M. L.; Toner, M. *J. Biomed. Mater. Res.* **1997**, *34*, 189−199.
(9) Khademhosseini, A.; Jon, S.; Suh, K. Y.; Tran, T. N. T.; Eng, G.; Yeh, J.; Seong, J.; Langer, R. *Adv. Mater.* **2003**, *15*, 1995−2000.
(10) Camelliti, P.; McCulloch, A. D.; Kohl, P. *Microsc. Microanal.* **2005**, *11*, 249−259.
(11) Khademhosseini, A.; Langer, R.; Borenstein, J.; Vacanti, J. P. *Proc. Natl. Acad. Sci. U.S.A.* **2006**, *103*, 2480−2487.
(12) Chen, Z. L.; Chen, W.; Yuan, B.; Xiao, L.; Liu, D. B.; Jin, Y.; Quan, B. G.; Wang, J. O.; Ibrahim, K.; Wang, Z.; Zhang, W.; Jiang, X. Y. *Langmuir* **2010**, *26*, 17790−17794.
(13) Wei, C. W.; Cheng, J. Y.; Young, T. H. *Biomed. Microdevices* **2006**, *8*, 65−71.
(14) Huh, D.; Matthews, B. D.; Mammoto, A.; Montoya-Zavala, M.; Hsin, H. Y.; Ingber, D. E. *Science* **2010**, *328*, 1662−1668.
(15) Huang, C. P.; Lu, J.; Seon, H.; Lee, A. P.; Flanagan, L. A.; Kim, H. Y.; Putnam, A. J.; Jeon, N. L. *Lab Chip* **2009**, *9*, 1740−1748.
(16) Khademhosseini, A.; Ferreira, L.; Blumling, J.; Yeh, J.; Karp, J. M.; Fukuda, J.; Langer, R. *Biomaterials* **2006**, *27*, 5968−5977.
(17) Ma, H. P.; Liu, T. J.; Qin, J. H.; Lin, B. C. *Electrophoresis* **2010**, *31*, 1599−1605.
(18) Li, Y.; Yuan, B.; Ji, H.; Han, D.; Chen, S. Q.; Tian, F.; Jiang, X. Y. *Angew. Chem., Int. Ed.* **2007**, *46*, 1094−1096.
(19) Chen, Z. L.; Li, Y.; Liu, W. W.; Zhang, D. Z.; Zhao, Y. Y.; Yuan, B.; Jiang, X. Y. *Angew. Chem., Int. Ed.* **2009**, *48*, 8303−8305.
(20) Wright, D.; Rajalingam, B.; Selvarasah, S.; Dokmeci, M. R.; Khademhosseini, A. *Lab Chip* **2007**, *7*, 1272−1279.
(21) Fukuda, J.; Khademhosseini, A.; Yeh, J.; Eng, G.; Cheng, J. J.; Farokhzad, O. C.; Langer, R. *Biomaterials* **2006**, *27*, 1479−1486.
(22) Kane, B. J.; Zinner, M. J.; Yarmush, M. L.; Toner, M. *Anal. Chem.* **2006**, *78*, 4291−4298.
(23) Hsiao, A. Y.; Torisawa, Y. S.; Tung, Y. C.; Sud, S.; Taichman, R. S.; Pienta, K. J.; Takayama, S. *Biomaterials* **2009**, *30*, 3020−3027.
(24) Torisawa, Y. S.; Mosadegh, B.; Luker, G. D.; Morell, M.; O'Shea, K. S.; Takayama, S. *Integr. Biol.* **2009**, *1*, 649−654.
(25) Sung, K. E.; Yang, N.; Pehlke, C.; Keely, P. J.; Eliceiri, K. W.; Friedl, A.; Beebe, D. J. *Integr. Biol.* **2011**, *3*, 439−450.
(26) Kaji, H.; Yokoi, T.; Kawashima, T.; Nishizawa, M. *Lab Chip* **2009**, *9*, 427−432.
(27) Kaji, H.; Yokoi, T.; Kawashima, T.; Nishizawa, M. *Lab Chip* **2010**, *10*, 2374−2379.
(28) Duffy, D. C.; McDonald, J. C.; Schueller, O. J. A.; Whitesides, G. M. *Anal. Chem.* **1998**, *70*, 4974−4984.
(29) Unger, M. A.; Chou, H. P.; Thorsen, T.; Scherer, A.; Quake, S. R. *Science* **2000**, *288*, 113−116.
(30) Paduch, R.; Walter-Croneck, A.; Zdzisinska, B.; Szuster-Ciesielska, A.; Kandefer-Szerszen, M. *Cell Biol. Int.* **2005**, *29*, 497−505.
(31) Mayor, R.; Carmona-Fontaine, C. *Trends Cell Biol* **2010**, *20*, 319−328.
(32) Abercrombie, M. *Nature* **1979**, *281*, 259−262.